Document downloaded from:

http://hdl.handle.net/10251/57833

This paper must be cited as:

Del Río García, AI.; García, C.; Fernández Sáez, J.; Molina Puerto, J.; Bonastre Cano, JA.; F. Cases (2015). Electrochemical treatment of solutions containing a recalcitrant dye. A way of using dimensionally adaptable catalytic fabrics. Industrial and engineering chemistry research. 54:6418-6429. doi:10,1021/acs.iecr.5b00590.

The final publication is available at

http://dx.doi.org/10.1021/acs.iecr.5b00590

Copyright American Chemical Society

Additional Information

This document is the Accepted Manuscript version of a Published Work that appeared in final form in
Industrial and Engineering Chemistry Research, copyright © American Chemical Society after peer review and technical editing by the publisher.
To access the final edited and published work see
http://dx.doi.org/10.1021/acs.iecr.5b00590

On the electrochemical treatment of solutions containing a recalcitrant dye. A way of using dimensionally adaptable catalytic fabrics.

*Ana Isabel del Río, Carolina García, Javier Fernández, Javier Molina, José Bonastre, Francisco Cases**

Departamento de Ingeniería Textil y Papelera, Escuela Politécnica Superior de Alcoy, Universitat Politècnica de València. Plaza Ferrándiz y Carbonell, s/n, 03801, Alcoy, Spain.

fjcases@txp.upv.es

Abstract

The objective of this work is to study the decolourization/degradation of reactive dye Remazol Black (RMZB) in sulphuric media. The electrochemical behavior was evaluated by Cyclic Voltammetry (CV) using platinum (Pt) and glassy carbon (GC) as working electrodes. Different electrolyses were performed potentioscally using Pt, activated carbon textile (ACT) and activated carbon textile electrocatalytically improved with dispersed Pt (Pt-ACT) with and without NaCl. The decolourization was studied by UV-Visible spectroscopy. High Performance Liquid Chromatography (HPLC) also permitted to confim the dye degradation. Specific applied charge (Q/AhL^{-1}) was evaluated and the efficiencies of the dye degradation were discussed in terms of Electrical Energy per Order ($E_{EO}/kWhm^{-3}order^{-1}$). Field Emission Scanning Electron Microscopy (FESEM) was used to observe the morphological differences of a Pt-ACT electrode before and after the electrolyses confirming that the corverage of dispersed Pt remains on the surface.

1. Introduction

From an average economic growth point of view, it is expected that industrial water requirements will increase from 800 billion m^3 in 2009 to 1500 billion m^3 by 2030. In the textile industry, only dyeing processes consume more than 100 L/kg of fabric processed. This generates wastewaters which create a range of problems such as: upsetting biological activity in aquatic life, toxic effects or decomposition in carcinogenic or mutagenic compounds, among others[1]. Considering the increasingly stringent regulations and legislation, there is a definite need to find a suitable wastewater treatment. Different treatments to decolourise and degrade dyeing wastewaters have then attracted increasing interest since the large majority of these dyes are not degradable in conventional wastewaters treatment plants[2]. Then, according to the dye wastewater composition[3] a wide range of methods have been developed: ozonation[4], advanced oxidation processes[5] or adsorption processes[6] whose advantages and disadvantages (Table 1).

Over the last 30 years, electrochemical treatments have been proposed as an attractive alternative where the dye structure and the correct choice of the electrode material represent important factor to take into account (Table 2).

The use of textiles as electrode material offers a large number of geometrical possibilities, a high effective area per geometric unit and the manufacturing processes are technically and economically more favourable than those for metal substrates. This great versatility opens a number of possibilities concerning the design of electrochemical cells. In addition to this, it is important to mention that the use of activated carbon (AC) as catalyst on its own for the electrochemical treatment is growing. Some of the advantages are: size and porosity,

chemical stability, corrosion and thermal resistance and good electrical conductivity[13]. This last property also provides the possibility of a direct modification of the surface by electrochemical procedures and therefore, the experimental conditions are easier to control[14,15]. This in turn means it is feasible to tailor the surface of AC's to optimise their performance for specific applications (Table 3).

This work is focused on studying the catalytic properties of an AC textile (ACT). For this purpose, Pt particles were directly dispersed onto bare AC textiles (Pt-ACT). The electrochemical behaviour of these electrodes and their use for the degradation/decolourization of a reactive dye were studied. Remazol Black (RMZB) has been chosen as a model textile reactive dye whose molecular structure is illustrated in Figure 1. The dye presents two reactive groups. Both are composed by one ethylsulphate group and one aromatic sulphonate group. This dye is included in the class of di-azo dyes. These two azo groups (-N=N-) and the rest of the aromatic structures are the responsible for the colour of the dye.

2. Experimental

2.1. Dye solutions

RMZB ($C_{26}H_{21}Na_4N_5O_{19}S_6$; M_w=991 g mol^{-1}; λ_{max}=599 nm) was kindly provided by Dystar and used as received. Dye solutions were prepared with ultra-pure water obtained from an Elix 3 Millipore-Milli-Q Advantage A10 system with a resistivity near to 18.2 MΩ cm. Voltammetric measurements were performed using 5.00 g dm^{-3} and 0.60 g dm^{-3} dye

concentrations in 49 g dm^{-3} H_2SO_4 for a clear observation of the redox peaks. When needed, solutions were deoxygenated by bubbling nitrogen (N_2 premier X50S). Later electrolyses were performed using 0.06 g dm^{-3} dye concentrations in 49 g dm^{-3} H_2SO_4, according to real concentrations in wastewaters[1]. When adding NaCl to the solutions the concentration was 0.30 g dm^{-3}.

2.2. Chemicals

All reagents were of analytical grade. The sulphuric acid (H_2SO_4) and hexachloroplatinic acid hexahydrate ($H_2PtCl_6 \cdot 6H_2O$) were purchased from Merck. NaCl was from Fluka and it was used to study the effect of chloride ions.

2.3. Electrodes. Pretreatment or preparation

2.3.1. CV analyses.

The first part of the voltammetric tests were done using a Pt wire (0.50 mm diameter, 99.99% purity, acquired from Engelhard-Clal) as working electrode (WE). This electrode was pretreated according to the method developed by Clavilier[20]. The next step consisted of a study with a 3 mm diameter GC electrode. GC electrodes were also pretreated by polishing the electrode with 1.0, 0.3 and 0.05 μm alumina slurry. Once characterised the GC electrode, Pt was dispersed on its surface according to the procedure commented in section 2.3.2. for the ACT electrodes.

In all cases, a stainless steel (SS) electrode was used as counter electrode (CE). The pretreatment for SS electrodes was described by del Río et al.[21]

2.3.2. Electrolyses

First, a Pt wire was employed as CE and WE. The pretreatment of Pt is described in section 2.3.1. In the second part, ACT and Pt-ACT electrodes were used. The company Carbongen S.A. (Spain) supplied the hydrophilic activated carbon fabric (ref. HST 1110). To discard the presence of impurities on the surface of the fabric, a previous analysis (not included) by FT-IR-ATR was carried out. The technical characteristics of the activated carbon textiles are reported in Table 4[22,23]. The ACT electrodes were prepared with strips 1 cm x 2 cm area cut from the textile. In order to ensure a proper electric contact between the textile samples and the 2 mm copper rods used as support, they were glued (the tip was flattened to improve the electrical contact) using CircuitWorks® conductive epoxy resin by Chemtronics®. The resin was hardened in an oven at 90 ºC and wrapped with Teflon® tape to protect it from the solution. The preparation of Pt-ACT was performed in 5.00 mmol dm^{-3} $H_2PtCl_6 \cdot 6H_2O$ in 49 g dm^{-3} H_2SO_4 aqueous solution. The dispersion of Pt onto the ACT surface was carried out potentiostatically from -0.25 V to 0.4 V at 10 mV s^{-1} during 20 scans with a stainless steel counter electrode and Ag/AgCl (KCl 3M) as reference electrode.

2.4. Electrochemical characterization. Cyclic Voltammetry

Voltammetric characterization was performed in a three electrode cell using either a Pt wire or a GC as WE, a cylindrical mesh SS electrode as CE and Ag/AgCl (KCl 3M) as RE. The system was an Eco-Chemie Autolab PGSTAT302 potentiostat/galvanostat at room temperature. The ohmic potential drop was compensated in the Autolab software (GPES). Measurements were carried within an operational range from -0.20 V to 0.87 V, 1.25 V and 1.50 V, with scan rates of 10 and 50 mV s^{-1}.

2.5. Electrolyses

The electrolyses were performed using a divided H-type cell so the reduction and the oxidation processes could be studied separately. For this purpose, a Nafion 117 (DuPont) cationic membrane was used. The studies were done with an Eco-Chemie Autolab PGSTAT302 potentiostat/galvanostat at room temperature and constant agitation. In the first part, the oxidation of RMZB at different potentials was evaluated using two Pt wires as cathode and anode. The electrolyses were performed potentiostatically at oxidation and reduction potentials, and also alternating these potentials for 60 s at each potential. All the electrolyses lasted 24 h. In the second part, the reduction of RMZB was studied with an ACT electrode as cathode (Pt wire as anode). Moreover, the oxidation of RMZB was studied with a Pt-ACT electrode as anode (Pt wire as cathode). The reference electrode was Ag/AgCl (KCl 3M). In all cases, the non-studied compartment was filled with 49 g dm^{-3} H_2SO_4. In some cases, NaCl was added to evaluate the effect of chloride ions. The working volume was 0.055 dm^{-3} and different samples were collected. The intensity, the charge, the potential difference and the electrode potential in blank solution compartment were also measured.

2.6. Analyses and instruments

HPLC analyses were performed with a Hitachi Elite Lachrom Chromatographic System equipped with diode array detector. The separations were performed on a Lichrospher 100RP-18C column (5 μm packing). The method used is that described by del Río et al.[24]. The detection wavelength (λ_{det}) was 600 nm and 310 nm. UV-Visible spectra were also

obtained with this system. This was possible changing the column by a tubular piece (without any packing inside). This allows the sample to flows to the detector.

To observe the morphology of the electrode surfaces, a Zeiss Ultra 55 FESEM was used (acceleration voltage: 3 kV).

3. Results and discussion

3.1. Cyclic Voltammetry

The electrode reactions characterizing the electrochemical behaviour of both the RMZB dye molecule and intermediates at the Pt electrode were studied by the dependence of the current on the electrode potential using the CV technique. Figure 2-a shows different voltammograms obtained for a 5 g dm^{-3} RMZB in 49 g dm^{-3} H_2SO_4 solution with Pt electrode as WE. The first scan was performed after maintaining constant the initial potential of the polarization program (-0.2 V) for 100 s (accumulation time). As can be seen, different redox processes appear. The most significant are the oxidation peaks observed at 0.22 V, 0.46 V and 0.61 V, and the reduction peaks at 0.15 V and 0.00 V. The second scan was performed without maintaining constant the initial potential. In general, it was observed that the intensity of the dye redox peaks decreased. The third scan was performed as the first one. The intensity of the peaks increased again which indicates that the intensity of these peaks is related to the accumulation time at the reduction potential. The fourth scan was performed in the same way as the first and third scans but bubbling N_2 after the accumulation time of -0.2 V. The majority of the redox processes of Pt disappeared, indicating that the dye species are not adsorbed on the surface because they

are easily removed from the vicinity of the electrode. They are generated in the vicinity of the electrode after an accumulation time at -0.20 V. The fifth scan was performed without bubbling N_2 and an increase of the intensity could be observed.

Figure 2-b shows different voltammograms corresponding to 5.00 g dm^{-3} RMZB in 49 g dm^{-3} H_2SO_4 on the Pt electrode when the higher potential limit was increased to 1.50 V. The first scan shows three oxidation peaks in the range of 0.87 V to 1.50 V. They could be attributed to the dye oxidation. Note that in the following scans the peak at 1.00V slightly disappears, in contrast with the other two peaks. Moreover, it was confirmed that higher potentials than 1.50 V produce the appearance of oxygen discharge (Figure 3).

These data were very important to assess the feasibility of the electrochemical process to degrade the RMZB molecule. The different electrolysis potentials were selected according to these voltammetric results.

The final objective of this work is the use of ACT electrodes in the degradation and decolourization process of solutions containing RMZB dye. Due to the nature of the ACT electrodes, the profile of the voltammograms does not present characteristic peaks. This is because of the high porosity of this materials which implies a high surface area. Moreover, it is difficult to control the area in contact with the solution during the voltammetric analysis. As a result, representative and reproducible voltammograms are not obtained. Therefore, the voltammetric peaks associated to the dye electrochemical behavour, which present a lower intensity and are ovelapped to the ACT response in the media, are poorly detected.

Then, the use of GC electrodes was considered for this characterization. One of the reasons is the easiness to obtain a reproducible surface after the previous pre-treatment which, obviously, allows to control the area. Besides, GC electrodes present an appropiate separation between the potential for the oxygen and hydrogen evolution.

Assuming these differences between GC and ACT electrodes, the results obtained were only considered to evaluate the potentials range of oxidation and reduction processes. These potentials were used as reference values in the potentiostatic electrolyses.

The voltammogram of 0.60 g dm^{-3} RMZB in 49 g dm^{-3} H_2SO_4 using GC is represented in Figure 2-c. Once again, in the forward scan an anodic peak around 1.00 V as shown in Figure 2-b was observed. In the reverse scan a cathodic peak at -0.10 V appeared. This peak was associated with the reduction of the RMZB molecule. In this potential range the supporting electrolyte showed no characteristic peaks other than the oxidation and reduction of the surface (dashed line in Figure 2-c). These processes are observed at around 0.50 V.

The voltammetric behaviour of 0.60 g dm^{-3} RMZB in 49 g dm^{-3} H_2SO_4 solution and 0.3 g dm^{-3} NaCl using a Pt-GC electrode was also studied. Figure 2-d shows the first scan (solid line) of the voltammogram obtained. As can be seen, an oxidation peak appeared around 1.40 V and its corresponding reduction peak at 1.20 V (reverse scan). This is associated to the dye electrochemical behaviour in the presence of chloride ions. The voltammogram corresponding to the blank solution (dashed line in Figure 2-d) also showed an oxidation peak near to 1.30 V related to the surface oxidation by chloride ions. Therefore, the oxidation peak at 1.40 V when performing the voltammetric test with the dye solution presents two contributions: the oxidation of the Pt-GC surface and the oxidation of the

RMZB molecule. In the absence of NaCl, the strong contribution of the surface oxidation overlaps the dye oxidation peak (figure not shown).

3.2. Electrochemical treatment of RMZB in a divided cell

The second part of this work consisted of the study of different controlled-potential electrolyses of 0.06 g dm^{-3} RMZB in 49 g dm^{-3} H_2SO_4. These electrolyses were conducted with and without NaCl.

3.2.1. Platinum electrode

As commented in Section 1, from the voltammetric results different anodic potentials were selected to study the degradation/decolourization degree of RMZB solutions. These values were in 1.20 V - 1.50 V range since at those values the voltammograms with Pt as working electrode presented two oxidation peaks.

3.2.1.1. UV-Visible spectroscopy and HPLC analyses

Figure 4 shows the UV-Visible spectra evolution for the different electrolyses. The initial spectrum showed that the wavelength of maximum absorbance (λ_{max}) in the Visible region was centred at 600 nm. According to the literature, this band is due to the long conjugated π system linked by two azo groups[25,26]. The cleavage of the two chromophore groups (R-N=N-R) takes place during the electrochemical treatment and this is the main reason which explains the increase of the decolourization. However, not all the electrolyses showed a complete decolourization after 24h of treatment. When the electrolysis was performed at a constant potential without NaCl (Figure 4-a and 4-b) the final solution only showed a

partial decolourization. This fact can be confirmed by means of the images inset in Figures 4-a and 4-b. On the other hand, as shown in Figures 4-c, 4-d, 4-e anc 4-f, the band at 600 nm diminished completely and the blue colour of the initial solution disappeared progressively. Data reported in the literature demonstrated that the yellowish colour of the final solution could be attributed to other by-product generated during the electrolysis[27-29]. According to our results, the kinetics of all the decolourization processes agreed whit a pseudo-first order. This means that the decolourization rate only depends on the initial dye concentration. The results are presented in Table 5. It was found that the decolourization rate of electrolyses performed at constant potential and in the absence of chloride (Figures 4-a and 4-b) was practically 3 times faster at 1.45 V than at 1.25 V. However, no complete decolourization was obtained in these cases, as commented before. It is also remarkable the improvement in 1.7 times when a constant potential of 1.45 V was applied and chloride was added to the solution. This explains the complete decolourization obtained in this case (Figure 4-d).

When cathodic and anodic potentials were applied alternatively (whether chloride is present in the solution or not), the decolourization rates were compared to that obtained at constant potential of 1.45 V without chloride. A significant increase from 1.8 times at worst case (-0.2 V and 1.25 V applied alternatively in the absence of chloride, Figure 4-c) to 4-5 times at best case (-0.2 V and 1.25 V or 1.45 V applied alternatively in the presence of chloride, Figures 4-e and 4-f) was found. Moreover, these decoloration rates are much more higher if we compare them with that obtained at 1.25 V without chloride (from 5 to 14 times higher). From these results, we can confirm that the applied potential and the presence of NaCl are determining factors for the decolourization degree.

In percentage terms, the decolourization achieved at constant potentials without chloride in the solution was 72 per cent and 96 per cent at 1.25 V and 1.45 V respectively, as shown in Table 5. Although these are percentages relatively high, the reason why there is a poor decolourization in these two cases is given by the molecular structure of RMZB. It is known that the dyeing process with this dye is more effective due to its two reactive groups (therefore, lesser quantities of dye are dumped). However, even low concentrations of this dye in wastewaters provide colour to wastewaters since the dye has two azo groups[30,31]. In fact, more than 24 hours are needed to obtain a complete decolourization at constant potential in the absence of chloride (Table 5).

On the contrary, the decolousation percentage of the rest of experiments were 99.9-100.

The changes observed in the UV also provides a significant information. Considering that the azo group is the first part of the RMZB to be degraded, the decrease of the bands located at 310 nm and 391 nm indicates the following bond-breaking of the aromatic structures. The first band corresponds to $\pi \rightarrow \pi^*$ transitions of the naphthelene rings and to the Ph-N=N or Ph-NH2 groups. The second one corresponds to the bond C-N located between the phenolic structure and the naphthalene structure[32-36]. Therefore, it would possible that two main intermediates were generated. On the one hand, an intermediate with naphthalene structure. On the second hand, a phenolic intermediate. The bands appeared at 254 nm and at 229 nm indicate the formation of phenolic compounds as a consequence of the additin of hydroxyl groups to the aromatic rings. This means that the opening of the aromatic rings occurs. Some authors have proposed a general pathway for the degradation of RMZB carried out by means of active anodes similar to Pt were

employed. In theses cases, they obtained the same naphtalenic and phenolic intermediates (with m/z 348 and 349 values, respectively) were detected but low minezalisation values were obtained. In addition to this, they also found that the kinetics and the formation of the intermediates depend on the applied potential and the electrolysis time[37-39].

In this work a low TOC removal was also abtained which agrees with the bibliography previously commented. This can be explained considering the nature of the electrodic material. Thus, it is interesant to highlight that Pt presents a high electrocatalytic activity towards the oxygen evolution reaction (OER). Therefore, Pt is included in the so-called category of "active electrodes", according the model proposed by Comninellis[40-44],. This model is based on the interaction established between the $^{\bullet}OH$ radicals generated during the oxidation of water and the electrode surface. This interaction is strongly favored to give the higher oxide PtO_{x+1} by reactions (1) and (2) respectively:

$$PtO_x + H2O \longrightarrow PtO_x(^{\bullet}OH) + H^+ + e^- \quad (1)$$

$$PtO_x(^{\bullet}OH) \longrightarrow PtO_x+1 + H^+ + e^- \quad (2)$$

The PtO_{x+1} is also able to participate in the oxidation reaction (reaction (3))

$$PtO_{x+1} + R \longrightarrow PtO_x + Products \quad (3)$$

Consequently, this leads to a low concentration of $^{\bullet}OH$ radicals on the Pt surface resulting in a selective oxidation of the dye and its intermediates. The reason is because the oxidising capacity of the higher oxide is weaker than that of $^{\bullet}OH$ radicals[44]. Taking this model into account, the low values of minezalisation seem to be reasonable.

The presence of chloride in solution implies a different mechanism for $^{\bullet}OH$ radicals generation which reflects the complexity of the process. The performance of the electrolyses can be significativly improved by using an inorganic mediator like "active chlorine". The quantity of $^{\bullet}OH$ radicals plays an important role on the generation of active chlorine from chloride during the electrolyses. Various proposals of mechanism for chlorine generation were given by several authors. Some of them were chronologically reviewed by S. Trasatti[45] who concluded that the most realistic mechanism was given by the adsorption of oxychloro-radicals. Thus, the reaction mechanism for chlorine generation takes into account the acid base equilibrium of the surface as the first step of the chlorine generation mechanism and it can be represented according to equations 4-8:

$$S{-}OH_2^+ \rightleftarrows S{-}(OH)_{ads} + H^+ \quad (4)$$

$$S{-}(OH)_{ads} \rightleftarrows S{-}O_{ads} + H^+ + e^- \quad (5)$$

$$S{-}O_{ads} + Cl^- \rightarrow S{-}(OCl)_{ads} + e^- \quad (6)$$

$$S{-}(OCl)_{ads} + Cl^- + H^+ \rightleftarrows S{-}(OH)_{ads} + Cl_2 \quad (7)$$

$$S{-}(OCl)_{ads} + Cl^- \rightleftarrows S{-}(O)_{ads} + Cl_2 + e^- \quad (8)$$

where S represents the active sites of the electrode surface.

In fact, lots of works have been published demonstrating that the chlorine is far much catalysed by an active anode such Pt[46,47]. Once generated chlorine, the following reactions take place on the bulk of the solution:

$$Cl_2 + H_2O \rightarrow HOCl + H^+ + Cl^- \quad (9)$$

$$HOCl \rightleftarrows H^+ + OCl^- \quad (10)$$

In our case, "active chlorine" was in the form of hypochloric acid since the pH of the solution was strongly acid.

Bonfatti and col.[48] demonstrated the great dependence of the degradation process on chloride concentration. The presence of a relatively small amount of chloride seems to inhibit the OER. This means that the potential required for the oxygen evolution increase since there is a higher reactivity of adsorbed hydroxyl and oxychloro radicals. The concentration of NaCl employed in this work is 0.3 g L^{-1} which could be considered a low value.

In addition to this, Panizza and col. [49] demonstrated that the presence of chloride also avoided the formation of a polymeric film on a Ti/Pt electrode. Obviously, this fact improved the performance of these electrodes for the treatment of industrial effluents containing several polyaromatic compounds. Martínez-Huitle et al.[50] also stated that the use of chlorides for the degradation of organic compounds changes the stoichiometry and microstructure of this film which also favours the degradation process increasing the OER potential. All this studies, together with the electrogeneration of the strong oxidants such as HClO and oxychloro compounds, as suggested Pourbaix diagrams, explain why the presence of chloride clearly improves the degradation and decolourization process.

In order to confirm the decolourization observed during the electrolysis, HPLC technique was employed. This technique is specifically useful to study the cleavage of the azo

structure as well as the formation of intermediates. The chromatographic peak corresponding to the dye before the treatment was detected at retention time (R_t) of around 12.0 minutes (λ_{det}=600 nm). The evolution of this peak with the electrolysis time confirmed the decolourization percentages presented in Table 5.

When λ_{det} was set at 310 nm, a main chromatographic peak (R_t=1.00 - 2.20 min) was detected in all cases indicating the low mineralization commented before.

3.2.1.2. Specific applied charge evolution (Q)

The evolution of the applied specific charge (Q/μAh mL^{-1}) versus time (h) was studied in all cases. It was found out that charge values of the electrolyses performed at a constant potential were lower than those registered when cathodic and anodic potentials were applied alternatively on the Pt electrode during the electrolysis. That is, the electrons exchange is higher in the cases with cathodic and anodic potentials were applied alternatively. A possible explanation could be that the electrode is partially blocked at a constant potential because of the presence intermediates formed in the vicinity of the electrode which are later adsorbed on the surface. Although the solution was continuously stirred, this fact was not enough for a proper diffusion of these species to the bulk solution. Therefore, continuous reduction and later oxidation (and vice versa) is necessary in order to the surface of the electrode does not get blocked. This behavior has been also observed with other dyes studied by our research group under similar conditions.

Moreover, the evolution of the exchange current on the electrode surface was measured versus time (Figure 5). Electrolyses performed at constant potential showed a decreasing

intensity along the electrolysis time until almost zero was reached. In contrast, electrolyses where reduction and oxidation potential were applied alternatively showed an increasing intensity which reveals a higher electronic exchange and so the electrolysis is more effective.

3.2.2. Activated carbon textile (ACT) and platinum modified activated carbon textile (Pt-ACT) electrodes.

Once the electrochemical treatment of RMZB was studied using a Pt wire as electrode, the degradation/decolourization was evaluated using and ACT electrode for electrochemical reduction process at -0.1 V and a Pt-ACT electrode for electrochemical oxidation at 1.45 V with NaCl. These potential were chosen

3.2.2.1. UV-Visible spectroscopy and HPLC analyses

Figures 6-a and 6-b show the results of colour removal and chromatographic information recorded at 600 nm obtained when a reduction potential of -0.10 V was chosen for an ACT electrode. Figures 6-c and 6-d show the same information when an oxidation potential of 1.45 V was applied in a Pt-ACT electrode. As revealed Figure 6-a, the electrochemical reduction led to complete colour removal and the band at 600 nm (azo groups) disappeared completely after 24h of electrolysis. Chromatographic analyses (Figure 6-b) also showed a complete disappearance of the dye peak at R_t=12.0 min.

When Pt-ACT electrode was used with NaCl, a shift of the absorbance in the Visible region to lower wavelengths was observed after the electrolysis (Figure 6-c) while the band at 600 nm disappeared completely. The residual colour of the final solution could be attributed to

new intermediates absorbing about 450 nm due to other types of chromophores. The elimination of the azo group was supported by HPLC analyses since the chromatographic peak at 12.0 min also disappeared (Figure 6-d). Rehorek et al. also observed this phenomenon for this dye[38].

In both cases, the bands in UV region diminish and were shifted which is attributed to the generation of aromatic intermediates whose structure is partially different from that of the RMZB molecule before the treatment.

The chromatographic results at a detection wavelength of 310 nm are presented in Figure 7. In the case of using an ACT electrode, after 24 hours of treatment three chromatographic peaks were observed at t_R between 1.5 and 3.0 minutes. In the corresponding UV-Vis spectrum (Figure 6-a), any band at 229 nm and 254 nm was observed which was related to the formation of phenolic intermediates. In contrast, the bands at 391 nm disappears. Moreover, the band at 310 nm is shifted as well as it partially diminishes. Therefore, it seems possible that during the reduction process carried out with an ACT electrode the azo group is reduced maybe by means of a hydrogenation of the double bond. This could explain the decolourization observed. According to this, aromatic amines could be generated without further degradation. The final dye solution resulting from the oxidation at 1.45 V with NaCl using a Pt-ACT electrode was also studied by HPLC at 310 nm (see Figure 7). In this case, similar chromatographic peaks were also observed at t_R between 1.5 and 3.0 minutes, where two of them presented higher intensity. This means that the concentration of the intermediates responsible for these peaks is higher. Taking into account the spectroscopical results showed in Figure 6-c, it could be feasible to consider the generation of phenolic intermediates since an intense band between 200 nm and 300 nm

appeared. This could be the result of the direct oxidation of $^{\bullet}OH$ radicals and the indirect oxidation of oxychloro compounds. It is also interesting to highllight that the same chromatographic peaks at 310 nm and the same spectroscopical changes in the UV region were also observed when the oxidation process was performed with a Pt as electrode at the same conditions (1.45 V with NaCl). Then, this could mean that the quantity of dispersed Pt on the ACT surface is appropiate to carry out these processes.

3.2.2.2. *Specific applied charge evolution (Q)*

Figure 8 represents the evolution of charge ($Q/\mu Ah\ mL^{-1}$) versus time of electrolysis (h) performed with the ACT electrode (Figure 8-a) and the Pt-ACT electrode in the presence of NaCl (Figure 8-b). When the ACT electrode was used a considerable increase in charge can be seen. In addition to this, the counter electrode potential was constant indicating the stability of the process. According to other works reported, functional groups like $–SO^{3-}$, $-COO^{-}$ and $–OH^{-}$ increase the solubility of reactive dyes[25]. Moreover, it has been demonstrated that they are not prone to being adsorbed. In these systems, the azo group is more susceptible to being reduced and yielding aromatic compounds as intermediates. Thus the result is a low (mineralization/decolourization) ratio. Therefore, when using the ACT electrode, the reduction of the azo group is the predominant step of the mechanism perhaps to generate aromatic amines responsible for the low mineralization. This low (mineralization/decolourization) ratio has been also reported by Shen et al.[51]. In case of using the Pt-ACT electrode, increasing charge values were also observed due to the greater catalytic surface because of the presence of platinum, although the presence of chloride also contributes to the better efficiency.

3.2.2.3. Electrical energy consumption

An important tool in evaluating the operating costs of electrochemical technologies is the electrical energy consumption. According to the international union of pure and applied chemistry (IUPAC), to estimate the electrical energy consumption not only the volume of the wastewater should be considered but also the concentration of the pollutant. With this purpose, the study of the kinetic order regime for high (processes that are overall zero order) and low concentrations (processes that are overall first order) is needed[52]. For high concentration of pollutants, the most appropriate parameter to evaluate the electrical energy consumption is the Electric Energy per Mass (E_{EM}/kWhkg^{-1}). This is defined as the electrical energy in kilowatt-hours (kWh) required to bring about the degradation of a unit mass of the contaminant (e.g. 1 kg) in polluted water or air and it is expressed by the following equation:

$$E_{EM} = \frac{P \cdot t \cdot 10^3}{V \cdot (c_i - c_f)} \quad (11)$$

where P is the rated power (kW), t is the time of electrolysis (h), V is the volume treated (L), c_i and c_f are the initial and final concentrations of the pollutant (g L^{-1}) of interest. The factor of 10^3 converts g to kg.

However, for low concentration of pollutants, which is the case of this work, the electric energy consumption is evaluated as Electric Energy per Order (E_{EO}/kWhm^{-3}). This parameter is defined as the electric energy in kilowatt-hours (kWh) required to degrade a contaminant by one of magnitude in a unit of volume (e.g. 1 m^3) of contaminated water or air. The corresponding equation is the following:

$$E_{E0} = \frac{P \cdot t \cdot 10^3}{V \cdot \log\left(\frac{c_i}{c_f}\right)} \quad (12)$$

where P is the rated power (kW), t is the time of electrolysis (h), V is the volume treated (m^3), c_i and c_f are the initial and final concentrations of the pollutant (g L^{-1}) of interest. In this case the factor of 10^3 converts L to m^3.

In the present study, the values of the dye concentration (g L^{-1}) remaining in solution after the electrolyses were difficult to measure since the percentages of the dye degradation were very high. However, the chromatographic peak associated to the chromophore group of the dye (absorbing at 600 nm) could be considered. This is because of the area of such peak is directly proportional to the concentration of dye whose chromophore group has not been degraded yet. Therefore, the area of this peak was used in eq. 2 instead of concentration and the corresponding equation is:

$$E_{E0} = \frac{P \cdot t \cdot 10^3}{V \cdot \log\left(\frac{A_i}{A_f}\right)} \quad (13)$$

where P, V and t have the same unities as in eq. (1) and (2). The logarithmic expression is dimensionless whatever the parameter was used (concentration or chromatographic area) so the use of the expression $log\ (A_i/A_f)$ should not be a problem.

The values of E_{EO} for both the electrolyses performed with the ACT electrode and Pt-ACT electrode in the presence of NaCl are presented in the Table 6. These data showed that the

electrochemical reduction performed with the ACT electrode required an electrical energy consumption two orders of magnitude less than that required for the oxidation with a Pt-ACT electrode with NaCl. From these results, it is reasonable to consider different degradation pathways for each case. Appart from this, as commented before, the low concentration of chloride present in solution implies an increase of electroactivity of the adsorbed hydroxyl and oxychloro radicals during the oxidation and the corresponding of increase of the anode potential. Therefore, the degradation of the dye is higher. This could explain the increase of the electrical consumption. However, according to the HPLC results, the intermediates generated after the oxidation with NaCl may not be as reactive as the initial dye molecule.

3.2.2.4. Field Emission Scanning Electron Microscopy (FESEM)

Figure 9 shows FESEM images of the Pt-ACT electrode before the electrolysis (Figure 9-a) and the same electrode after the electrolysis performed with chloride present in solution (Figure 9-b). Figure 9-c shows a magnified image of the Pt-ACT surface before the treatment. Figure 9-d shows a magnified image of this electrode after the treatment. These images clearly illustrate that platinum particles are homogeneously dispersed before the treatment. After the electrolysis, practically 100 per cent of Pt particles remains on the surface. In fact, EDX analyses demonstrated that the atomic percentage of Pt was around 3 per cent before and after the treatment. Moreover, after the treatment an increase of 80 per cent in atomic chlorine was found which confirms the indirect oxidation associated to chloride in solution.

4. Conclusions

The ACT and Pt-ACT electrodes showed good electrocatalytic activity. This characteristic makes them suitable for the electrochemical treatment of a reactive dye such as RMZB. From the voltammetric tests, it can be concluded that the initial accumulation time at reduction potential favours the formation of non-adsorbed intermediates. Moreover, the presence of chloride ions is also a determining factor in the electrochemical treatment. From the initial study with Pt electrodes, it has been proved that the decolourization obtained at constant potential without NaCl was not complete. At these potential conditions, the chromophore groups were destroyed only when NaCl was added to the dye solution, due to the indirect oxidation, as UV-Visible spectroscopy and HPLC revealed. However, the electrolyses where reduction and oxidation potentials were applied alternatively gave much better decolourization results with values of specific charge two orders of magnitude higher. UV-Visible and HPLC also revealed a low mineralization in all cases with some intermediates absorbing in the Visible region. In all cases followed a kinetic of pseudo-first order. The low mineralization was also confirmed for ACT and Pt-ACT electrodes at conditions of reduction and oxidation, respectively. However, the decolourization obtained was better in the case of the reduction with ACT electrodes. To oxidise the RMZB molecule, it is necessary to modify the ACT surface with dispersed platinum. In this case, some of the intermediates generated during the oxidation could be responsible for the residual colour. In general terms, the use of both ACT and Pt-ACT electrodes in potentiostatic electrolyses presents high and increasing charge values,

although in the case of ACT the electrical energy consumption was lower. This could be associated to the different pathways of both reduction and oxidation procesess.

In conclusion, due to the versatility of ACT and Pt-ACT electrodes, it is apparent that this method can be adapted for application in an electrolysis system of wastewater coming from textile industry. Currently, more work is in progress in the design and adaptability of a new reactor with a higher capacity for the treatment of these dye solutions using these electrodes. Moreover, this treatment is being studied with other reactive dyes.

Achknowlegements

Authors wish to thank to the Spanish Ministerio de Ciencia e Innovación (contract CTM2011-23583 and CTM2014-52990-R) and Universitat Politècnica de València (Vicerrectorado de Investigación PAID-06-10 contract 003-233) for the financial support. A.I. del Río is grateful to the Spanish Ministerio de Ciencia y Tecnología for her FPI fellowship. J. Molina is grateful to the Conselleria d'Educació, Formació i Ocupació (Generalitat Valenciana) for the Program VALi+D Postdoctoral Fellowship. C. García is grateful to the Conselleria d'Educació, Formació i Ocupació (Generalitat Valenciana) for her Gerónimo Forteza fellowship.

Table 1

Main characteristics of textile waswaters and advantages and disadvantages of different treatments for textile wastewater

Character	Value
Total Suspended Solid (TSS mg dm^{-3})	34
Total organic carbon (TOC, mg dm^{-3})	1810
BOD_5 (mg dm^{-3})	1540
COD (mg dm^{-3})	3325
pH	11.82
Color (ADMI units)	41530
Total Kjeldahl nitrogen (TKN, mg dm^{-3})	314
Chloride (mg dm^{-3})	24200

Process	Advantages	Disadvantages
Biodegradation	Rates of elimination by oxidisable substances about 90%	Low biodegradability of dyes
		Costs
Coagulation–flocculation	Elimination of insoluble dyes	Production of sludges
		Costs
Adsorption on activated carbon	Suspended solids and organic substances well reduced	Blocking filter
Ozone treatment	Good decolorization	No reduction of the COD
		Additional costs
Reverse osmosis	Removal of all mineral salts, hydrolyzed reactive dyes and chemical auxiliaries	Iron hydroxide sludges
Nanofiltration	Separation of organic compounds of low molecular weight and divalent ions from monovalent salts	High pressure
	Treatment of high concentrations	
Ultrafiltration–microfiltration	Low pressure	Insufficient quality of the treated wastewater

Table 2

Electrochemical oxidation processes with different electrodes

Electrode	Dye	I (mA cm^{-2}) / E(V)	Electrolysis time (h)	% Decolourisation	Energy Consumption	Ref.
Pt	Amaranth (Acid Red 27)	10 – 20 mA cm^{-2}	3	100	----	(7)
BDD	Direct red 80	1.5 mA cm^{-2}	24	100	6.65 kWh m^{-3}	(8)
Graphite	Vat Blue (Indigo)	5 V 30 g dm^{-3} NaCl	2	90	1.84 kWh m^{-3}	(9)
Pt	Reactive Orange 4 (PMX2R)	40 mA cm^{-2}	1	91	44.1 kWh m^{-3}	(10)
Ti/RuO_2	Procion Black (Acid Blue)	10 mA cm^{-2}	90 min	Unkown	61.3 kWh (g COD)$^{-1}$	(11)
ACF	Amaranth (Acid red 27)	0.5 mA cm^{-2}	8	99	----	(12)

Table 3

AC-catalysed decolourisation of different dyes.

Process	Dye	Anode Cathode	BET (m^2 g^{-1})	% Decolourisation	Ref.
Electrochemical Oxidation	Alizarin Red S	Viscose-based ACF SS	1000	98	(16)
Electrochemical Oxidation	Alizarin Red S	Viscose-based ACF SS	1682	82	(17)
Electrochemical Oxidation	Acid Red 14	Ru_2Ti ACF	1237	---	(18)
Electrochemical Oxidation	Acid Orange 4	SS ACF	764.1	96	(19)

Table 4

Characterization parameters of the activated carbon textile used in the present work.

Parameters	Units	Values
Weigth	$g\ m^{-2}$	105 ± 5
BET[a]	$m^2\ g^{-1}$	1,100 ± 100
Iodine Index[b]	mg $I_2\ g^{-1}$	1,100 ± 50
Permeability[c]	$mm\ s^{-1}$	728 ± 44
Thickness[d]	mm	0.505 ± 0.016
Tensile strength[e] warp	N	230 ± 23
Tensile strength[e] weft	N	120 ± 18
Elongation strength[e] warp	%	4.60 ± 1.19
Elomgation strength[e] weft	%	8.28 ± 0.40
LOI[f]	%	48

[a] BET Brunauer, Emmet, and Teller. Results got applying this statistical equation to JVJ isotherm adsorption at -196 ℃
[b] ASTM D 4607-86 modified using photometric determination
[c] UME EN ISO 9237:1999
[d] UNE EN ISO 5084:1997
[e] UNE EN ISO 13934-1:1999
[f] UNE EN ISO 4589-2:2001

Table 5

Decolorourization rate of the electrolyses performed with a platinum electrode, time to achieve a decolourization of 99 per cent and decolourization

WE potential (V)	Electrolyte	k^{-1}	R^2	$t(h)_{decol\ 99\%}$	Decolourisation percentage $_{24\ h}$
1,25	Na_2SO_4 0,5 M	-0,05	0,94	88,09	71,84
1,45	Na_2SO_4 0,5 M	-0,15	0,91	31,89	96,62
-0,20 ↔ 1,25	Na_2SO_4 0,5 M	-0,27	0,93	18,26	99,79
1,45	Na_2SO_4 0,5 M + NaCl $5 \cdot 10^{-3}$ M	-0,26	0,80	17,62	99,80
-0,20 ↔ 1,25	Na_2SO_4 0,5 M + NaCl $5 \cdot 10^{-3}$ M	-0,75	0,91	6,94	100,00
-0,20 ↔ 1,45	Na_2SO_4 0,5 M + NaCl $5 \cdot 10^{-3}$ M	-0,59	0,98	8,20	100,00

Table 6

Electrical energy per order (EEO) for the electrochemical reduction of 0.06 g dm-3 RMZB in 49 g dm-3 H2SO4 at -0.10 V using an ACT electroce (left) and for the electrochemical oxidation at 1.45 V using a Pt-ACT electroce (right). Time of electrolysis: 24h.

Electrical energy per order (kWh m^{-3})	
ACT electrode	Pt-ACT electrode
1.66 E-03	3.92 E-01

References

(1) Zaharia, C.; Suteu, D. *Textile Organic Dyes – Characteristics, Polluting Effects and Separation/Elimination Procedures from Industrial Effluentes-A Critical Overview, in Organic Pollutants Ten Years After the Stockholm Convention – Environmental and Analytical Update*; InTech: Europe, 2012.

(2) Martínez-Huitle, C.A.; Brillas, E.; Decontamination of wastewaters containing synthetic organic dyes by electrochemical methods: A general review. *Appl. Catal. B Environmental*. **2009**, *87*, 105.

(3) Vlyssides, A.G.; Loizidou, M.; Karlis, P.K.; Zorpas, A.A.; Papaioannou, D. Electrochemical oxidation of a textile dye wastewater using a Pt/Ti electrode. *J. Hazard. Mater.* **1999**, *70,* 41.

(4) Wang, C.; Yediler A.; Lienert, Z.; Wang, Z.; Kettrup, A. Ozonation of an azo dye C.I. Remazol Black 5 and toxicological assessment of its oxidation products. *Chemosphere* **2003**, *52*, 1225.

(5) Swaminathan, K.; Sandhya, S.; Carmalin, S.A.; Pachhade, K.; Subrahmanyam, Y.V. Decolorization and degradation of H-acid and other dyes using ferrous-hydrogen peroxide system. *Chemosphere* **2003**, *50,* 619.

(6) Dávila-Jiménez, M.M.; Elizalde-González, M.O.; Peláez-Cid, A.A. Adsorption interaction between natural adsorbents and textile dyes in aqueous solution. *Colloids Surf. A*. **2005**, *254*, 107.

(7) Hattori, S.; Doi, M.; Takahashi, E.; Kurosu, T.; Nara, M.; Nakamatsu, S.; Nishiki, Y.; Furuta, T.; Iida, M. Electrolytic decomposition of Amaranth dyestuff using diamond electrodes. *J. Appl. Electrochem.* **2003**, *33*, 85.

(8) Lopes, A.; Martins, S.; Morao, A.; Magrinho, M.; Goncalves, I. Degradation of a Textile Dye C. I. Direct Red 80 by Electrochemical Processes. *Port. Electrochim. Acta* **2004**, *22*, 279.

(9) Cameselle, C.; Pazos, M.; Sanromán, M.A. Selection of an electrolyte to enhance the electrochemical decolourisation of indigo. Optimisation and scale-up. *Chemosphere* **2005**, *60*, 1080.

(10) López-Grimau, V.; Gutiérrez, M.C. Decolourisation of simulated reactive dyebath effluents by electrochemical oxidation assisted by UV light. *Chemosphere* **2006**, *62*, 106.

(11) Mohan, N.; Balasubramanian, N.; Subramanian, V. Electrochemical Treatment of Simulated Textile Effluent. *Chem. Eng. Technol.* **2001**, *24*, 749.

(12) Fan, L.; Zhou, Y.; Yang, W.; Chen, G.; Yang, F.; Electrochemical degradation of Amaranth aqueous solution on ACF. *J. Hazard. Mater.* **2006**, *B137,* 1182.

(13) Marsh, H.; Reinoso, F.R. *Sciences of Carbon Materials*; Publicaciones de la Universidad de Alicante: Alicante, 2000.

(14) Molina, J.; Del Río, A.I.; Bonastre, J.; Cases, F. Chemical and electrochemical polimerisation of pyrrole on polyester textiles in presence of phosphotungstic acid. *Eur. Polym. J* **2008**, *44*, 2087.

(15) Molina, J.; Esteves, M.F.; Fernández, J.; Bonastre, J.; Cases, F. Polyaniline coated conducting fabrics. Chemical and electrochemical characterization. *Eur. Polym. J.* **2011**, *47*, 2003.

(16) Yi, F.; Chen, S. Electrochemical treatment of alizarin red S dye wastewater using an activated carbon fiber as anode material. *J. Porous Mat.* **2008** *15*, 565.

(17) Yi, F.; Chen, S.; Yuan, C. Effect of activated carbon fiber anode structure and electrolysis conditions on electrochemical degradation of dye wastewater. *J. Hazard. Mater.* **2008**, *157,* 79.

(18) Wang, A.; Qu, J.; Ru, J.; Liu, H.; Ge, J. Mineralization of an azo dye Acid Red 14 by electro-Fenton's reagent using an activated carbon fiber cathode. *Dyes Pigments* **2005**, *65*, 227.

(19) Xu, L.; Zhao, H.; Shi, S.; Zhang, G.; Ni, J. Electrolytic treatment of C.I. Acid Orange 7 in aqueous solution using a three-dimensional electrode reactor. *Dyes Pigments* **2008**, *77*, 158.

(20) Clavilier, J. The role of anion on the electrochemical behaviour of a {111} platinum surface; an unusual splitting of the voltammogram in the hydrogen region. *J. Electroanal. Chem.* **1979**, *107*, 211.

(21) Del Río, A.I.; Molina, J.; Bonastre, J.; Cases, F. Influence of electrochemical reduction and oxidation processes on the decolourisation and degradation of C.I. Reactive Orange 4 solutions. *Chemosphere* **2009**, *75*, 1329.

(22) Fernández, J.; del Río, A.I.; Molina, J.; Bonastre, J.; Cases, F. Modified carbon fabrics electrodes: preparation and electrochemical behavior toward amaranth electrolysis. *J. Appl. Electrochem*. **2015,** *45,* 263.

(23) Fernández, J.; Molina, J.; del Río, A.I.; Bonastre, J.; Cases, F. Synthesis and characterization of electrochemically platinum-polyaniline modified carbon textile electrodes. *Int. J. Electrochem. Sci*. **2012**, *7*, 10175.

(24) Del Río, A.I.; Benimeli, M.J.; Molina, J.; Bonastre, J.; Cases, F. Electrochemical Treatment of C.I. Reactive Black 5 Solutions on Stabilized Doped Ti/SnO_2 Electrodes. *Int. J. Electrochem. Sci*. **2012**, *7*, 13074.

(25) Silverstein, R.M.C; Basdler, G.C.; Morrill, G.C. *Spectrophotometric Identification of organic compounds*; Wiley: New York, 1991.

(26) Feng, J.; Hu, X.; Yue, P.L.; Zhu, H.Y.; Lu, G.Q. Discoloration and mineralization of Reactive Red HE-3B by heterogeneous photo-Fenton reaction. *Water Res.* **2003**, *37*, 3776.

(27) Rehorek, A.; Plum, A.; Strategies for continuous on-line high performance liquid chromatography coupled with diode array detection and electrospray tandem mass spectrometry for process monitoring of sulphonated azo dyes and their intermediates in anaerobic–aerobic bioreactors. *J. Chromatogr. A*. **2005**, *1084*, 119.

(28) Pham, T.L.H.; Weisshoff, H.; Mügge, C.; Krause, E.; Rotard, W.; Preiss, A.; Zaspel, I. Non-Target-Analytik in der Ökologie. *Mitt. Umweltchem. Ökotox.* **2010**, *1*, 2.

(29) Méndez-Martínez,, A.J.; Dávila-Jiménez, M.M.; Ornelas-Dávila, O.; Elizalde-González, M.P.; Arroyo-Abad, U.; Sirés, I.; Brillas, E. Electrochemical reduction and oxidation pathways for Reactive Black 5 dye using nickel electrodes in divided and undivided cells. *Electrochim. Acta* **2012**, *59*, 140.

(30) Crespi, M.; Tecnología disponible para disminuir la contaminación de los efluentes textiles. *Revista Química Textil* 1**994**, *177*, 36.

(31) Integrated Pollution Prevention and Control (IPPC). Reference Document on Best Available Techniques for the Textile Industry. July 2003. European Commission

(32) Yang, J. *Analysis of Dye*; Chemical Industry Press: Beijing, 1987.

(33) Feng, W.; Nansheng, D.; Helin, H. Degradation mechanism of azo dye C. I. reactive red 2 by iron powder reduction and photooxidation in aqueous solutions. *Chemosphere* **2000**, *41*, 1233.

(34) Galindo, C.; Jacques, P.; Kalt, A. Photodegradation of the aminoazobenzene acid orange 52 by three advanced oxidation processes: UV/H_2O_2, UV/TiO_2 and VIS/TiO2 Comparative mechanistic and kinetic investigations. *J. Photochem. Photobiol. A: Chem.* **2000**, *130*, 35.

(35) Stylidi, M.; Kondarides, D.I.; Verykios, X.E. Visible light-induced photocatalytic degradation of Acid Orange 7 in aqueous TiO_2 suspensions. *Appl. Catal. B: Environ.* **2004**, *47*, 189

(36) Sahel, K.; Perol, N.; Bordes, C.; Derriche, Z.; Guillard, C. Photocalytic decolorization of Remazol Black (RB5) and Procion MX-5B – Isotherm of adsorption, kinetic of decolorization and mineralization. *Appl. Catal. B Environmental.* **2007**, *77*, 100.

(37) Méndez-Martínez, A.J.; Dávila-Jiménez, M.M.; Ornelas-Dávila, O.; Elizalde-Gonzñalez, M.P.; Arroyo-Abad, U.; Sirés, I.; Brillas, E. Electrochemical reduction and oxidation pathways for Reactive Black 5 using nickel electrodes in divided and undivided cells. *Electrochim. Acta.* **2012**, *59*, 140.

(38) Rehorek, A.; Plum, A. Online LC-MS-MS process monitoring for optimization of biological treatment of wastewater containing azo dye concentrates. *Anal. Bioanal. Chem*. **2006**, *384*, 1123.

(39) Lucas, M.S.; Peres, J.A. Decolorization of the azo dye Reactive Black 5 by Fenton and photo-Fenton oxidation. *Dyes Pigments* **2006**, *71*, 236.

(40) Comninellis, Ch.; Plattner, E. Electrochemical wastewater treatment. *Chimia.* **1988**, *42*, 250.

(41) Comninellis, Ch.; Pulgarin, C. Anodic oxidation of phenol for waste water treatment. *J. Appl. Electrochem*. **1991**, *21*, 703.

(42) Comninellis, Ch. Electrochemical treatment of wastewater. *Gas Wasser Abwasser*. **1992**, *72*, 792.

(43) Comninellis, Ch.; Pulgarin, C. Electrochemical oxidation of phenol for wastewater treatment using SnO_2 anodes. *J. Appl. Electrochem.* **1993**, *23*, 108.

(44) Comninellis, Ch. Electrocatalysis in the electrochemical conversion/combustion of organic pollutants for waste water treatment. *Electrochim. Acta.* **1994**, *39*, 1857.

(45) Trasatti, S. Progress in the understanding of the mechanism of chlorine evolution at oxide electrodes. Electrochim. Acta 1987, 32, 369.

(46) Vlyssides, A.G.; Karlis, P.K.; Zorpas, A.A.; Electrochemical treatment in relation to pH of domestic wastewater using Ti/Pt electrodes. *J. Hazard. Mater. B* **2002**, *95*, 215.

(47) Sakalis, A.; Mpoulmpasakos, K.; Nickel, U.; Fytianos, K.; Voulgaropoulos, A. Evaluation of a novel electrochemical pilot plant process for azo dyes removal from textile wastewater. *Chem. Eng. J.* **2005**, *111*, 63.

(48) Bonfatti, F.; De Battisti, A. ; Ferro, S.; Lodi, G.; Osti, S. Anodic mineralization of organic substrates in chloride-containing aqueous media. *Electrochim. Acta* **2000**, *46*, 305.

(49) Panizza, M.; Bocca, C.; Cerisola, G. Electrochemical treatment of wastewater containing polyaromatic organic pollutants. *Wat. Res.* **2000**, *34*, 2601.

(50) Martínez-Huitle, C.A.; Ferro, S.; De Battisti, A. Electrochemical Incineration in the Presence of Halides. *Electrochem. Solid-State Lett*. **2005**, *8*, D35.

(51) Shen, Z.; Wang, W.; Jia, J.; Ye, J.; Feng, X.; Peng, A. Degradation of dye solution by an activated carbon fiber electrode electrolysis system. *J. Hazard. Mater. B*. **2001**, *84*, 107.

(52) Bolton, J.R.; Bircher, K.G.; Tumas, W.; Tolman, C.A. Figures-of-merit for the technical development and application of advanced oxidation technologies for both electric- and solar-driven systems. *Pure Appl. Chem.* **2001**, *73*, 627.

Generic name (Colour Index)	Strtuctural chracteristics	Molecular weight (g mol^{-1})	Supplier	λ_{max} (nm)
Reactive Black 5 (Colour Index 20505)	Di-azo dye Two aromatic sulphonate groups Two ethyl sulphate groups	991.8	DyStar	Visible region: 600 nm UV region: 310 nm

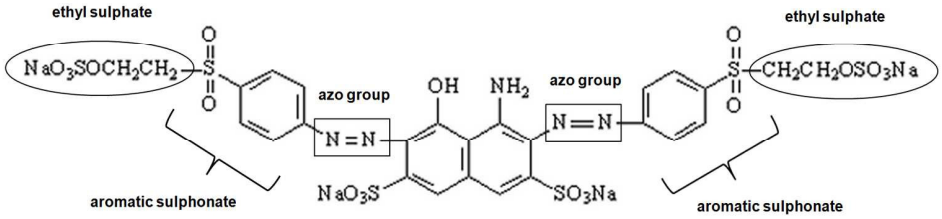

Figure 1 Chemical structure and main properties of RMZB.
148x58mm (300 x 300 DPI)

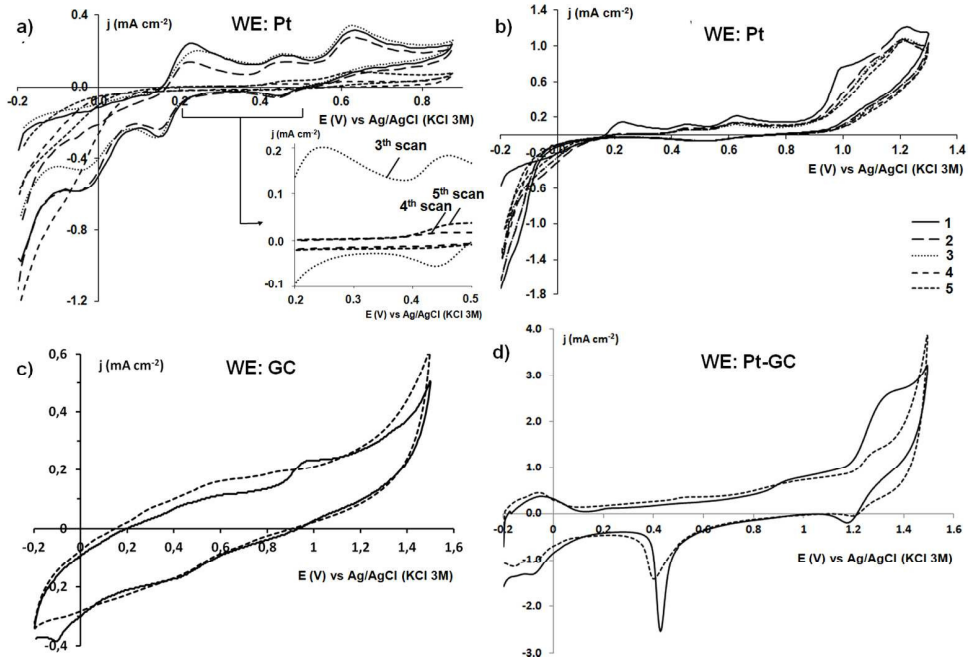

Figure 2 Cyclic voltammograms of 5.00 g dm-3 RMZB in 49 g dm-3 H2SO4 without NaCl (a, b), 0.60 g dm-3 RMZB in 49 gl dm-3 H2SO4 (c) and 0.60 g dm-3 RMZB in 49 gl dm-3 H2SO4 with 0.30 g dm-3 NaCl (d). Polarisation conditions: a) WE: Pt; from -0.20 V to 0.87 V; 1st scan: 100 s at -0.20 V (—), 2nd scan: normal (— —); 3rd scan: 100 s at -0.20 V (•••••); 4th scan: 100 s at -0.20 V and bubbling N2 (– – –); 5th scan: normal (- - -); 50 mV s-1 b) WE: Pt; from -0.20 V to 1.50 V; 1st scan: (—); 2nd scan: (— —); 3rd scan: (•••••); 4th scan: (– – –); 5th scan: (- - -); 50 mV s-1 c) WE: GC; from -0.20 V to 1.50 V; 10 mV s-1; RMZB solution (—) and blank solution (– – –); 10 mV s-1 d) WE: Pt-GC; from -0.20 V to 1.50 V; 10 mV s-1; RMZB (—) and blank solution (– – –); 10 mV s-1.
136x92mm (300 x 300 DPI)

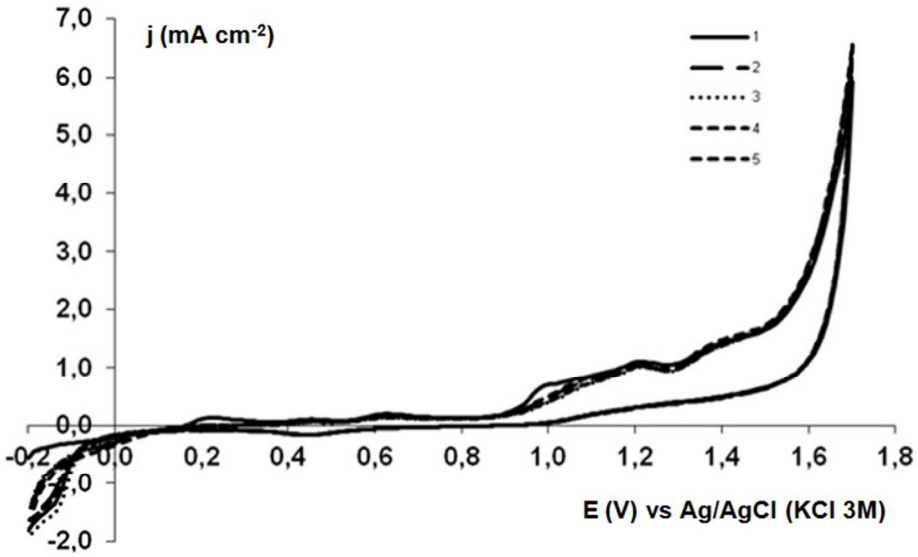

Figure 3 Cyclic voltammograms of 5.00 g dm-3 RMZB in 49 g dm-3 H2SO4. Polarisation conditions: a) WE: Pt; from -0.20 V to 1.7 V.
70x42mm (300 x 300 DPI)

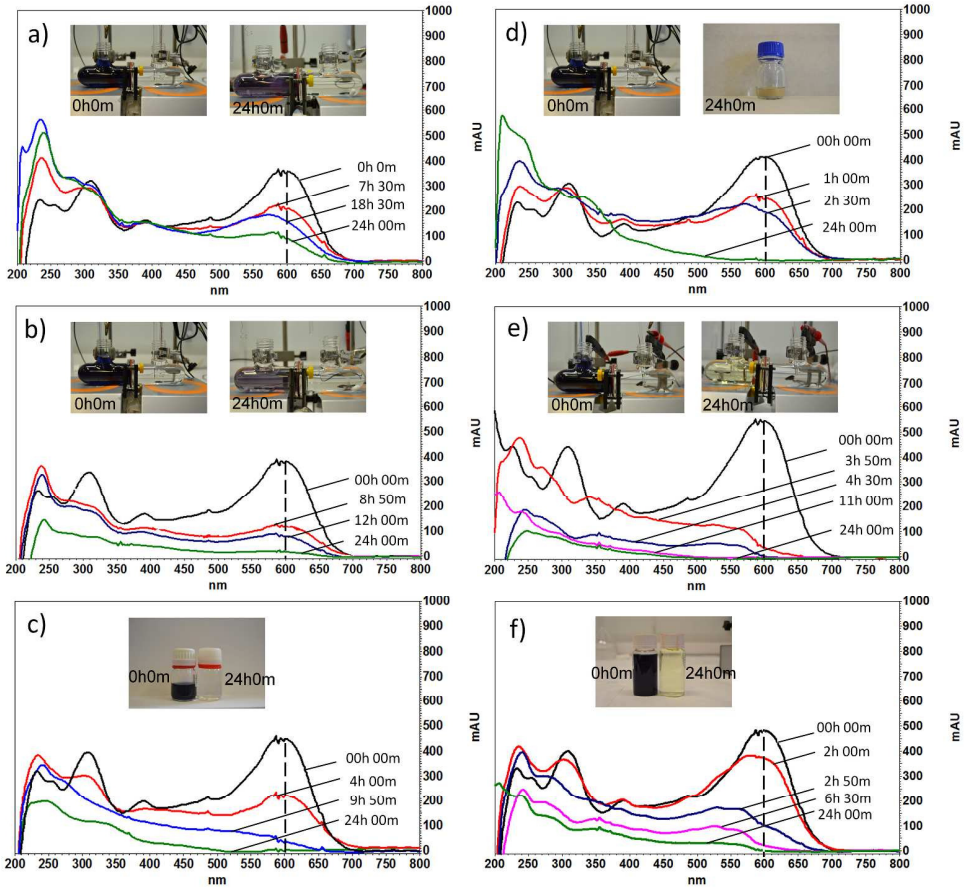

Figure 4 UV-Visible spectra evolution of 0.06 g dm-3 RMZB in 0.50 mol dm-3 H2SO4 during the electrochemical treatment. Anode and cathode: Pt in all cases. Potential conditions: a) 1.25 V without NaCl; b) 1.45 V without NaCl; c) -0.20 V and 1.25 V alternatively, without NaCl; d) 1.45 V with 0.30 g dm-3 NaCl; e) -0.20 V and 1.25 V alternatively, with 0.30 g dm-3 NaCl; f) -0.20 V and 1.45 V alternatively, with 0.30 g dm-3 NaCl. Inset figures: colour of the dye solution before and after the treatment. Potential conditions: a) 1.25 V without NaCl; b) 1.45 V without NaCl; c) -0.20 V and 1.25 V alternatively, without NaCl; d) 1.45 V with 0.30 g dm-3 NaCl; e) -0.20 V and 1.25 V alternatively, with 0.30 g dm-3 NaCl; f) -0.20 V and 1.45 V alternatively, with 0.30 g dm-3 NaCl. Inset figures: colour of the dye solution before and after the treatment.
131x121mm (600 x 600 DPI)

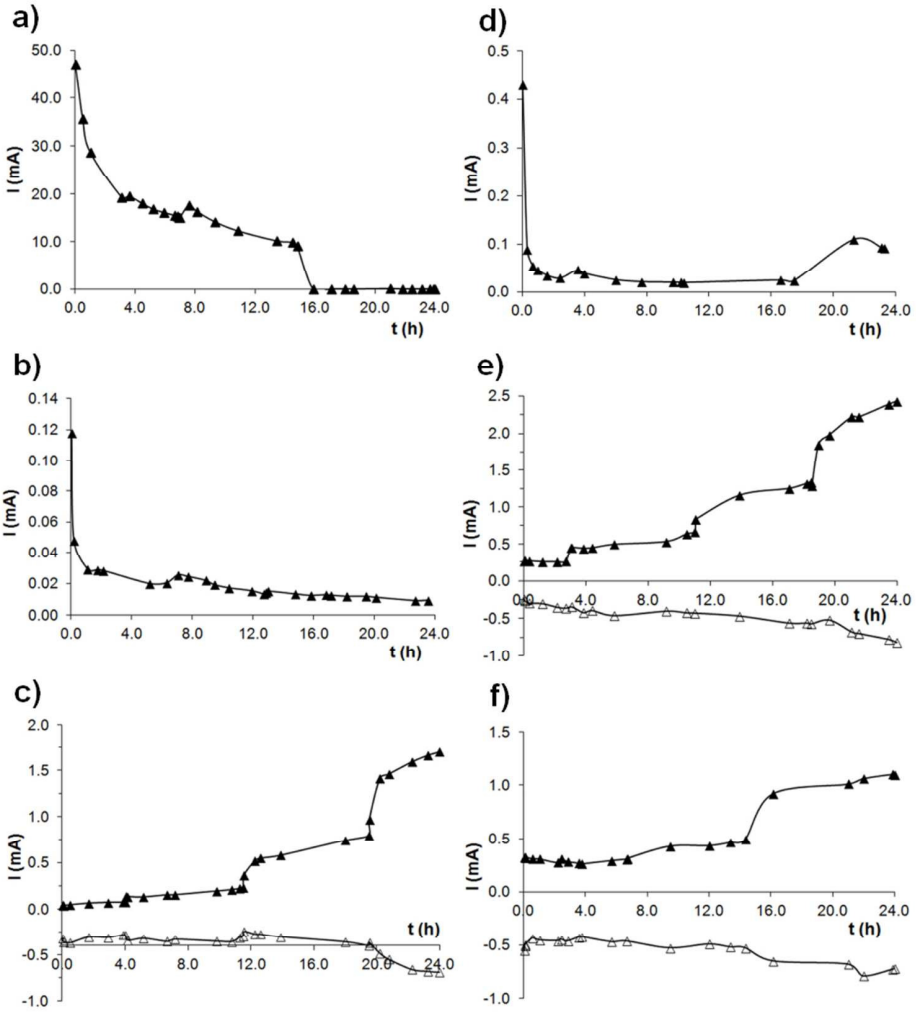

Figure 5 Evolution of current versus time of electrolysis. Anode and cathode: Pt in all cases. Potential conditions: a) 1.25 V without NaCl; b) 1.45 V without NaCl; c) -0.20 V and 1.25 V alternatively, without NaCl; d) 1.45 V with 0.30 g dm-3 NaCl; e) -0.20 V and 1.25 V alternatively, with 0.30 g dm-3 NaCl; f) -0.20 V and 1.45 V alternatively, with 0.30 g dm-3 NaCl.
83x90mm (300 x 300 DPI)

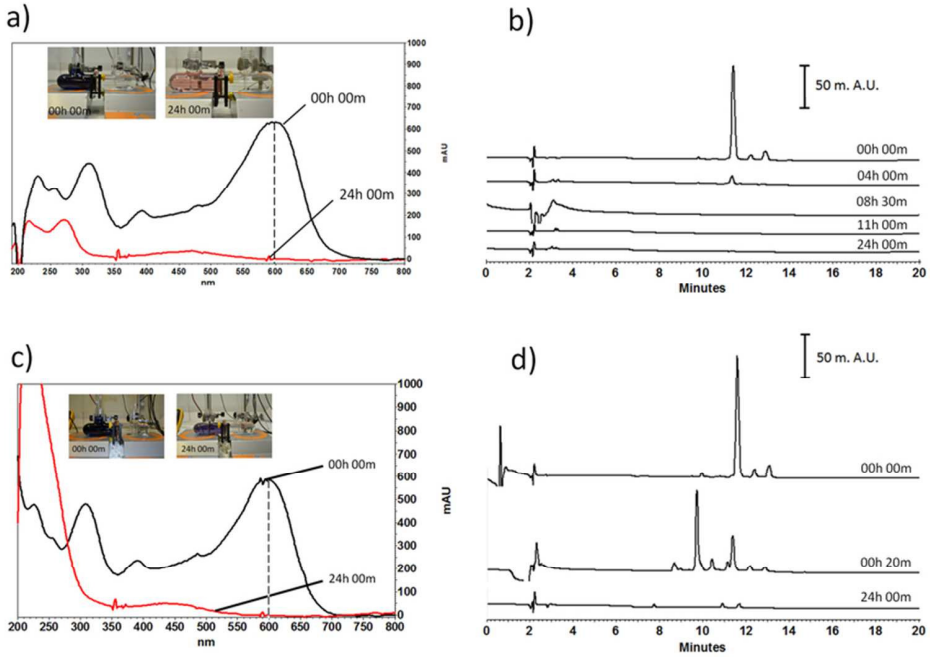

Figure 6 a) UV-Vis spectra before and after the electrolysis with an ACT electrode at -0.10 V; b) chromatographic evolution recorded at 600 nm during the electrolysis with an ACT electrode at -0.10 V; c) UV-Vis spectra before and after the electrolysis with a Pt-ACT electrode at 1.45 V in the presence of NaCl; d) chromatographic evolution recorded at 600 nm during the electrolysis with a Pt-ACT electrode at 1.45 V in the presence of NaCl. Inset images: colour of the initial and final solution.
74x51mm (300 x 300 DPI)

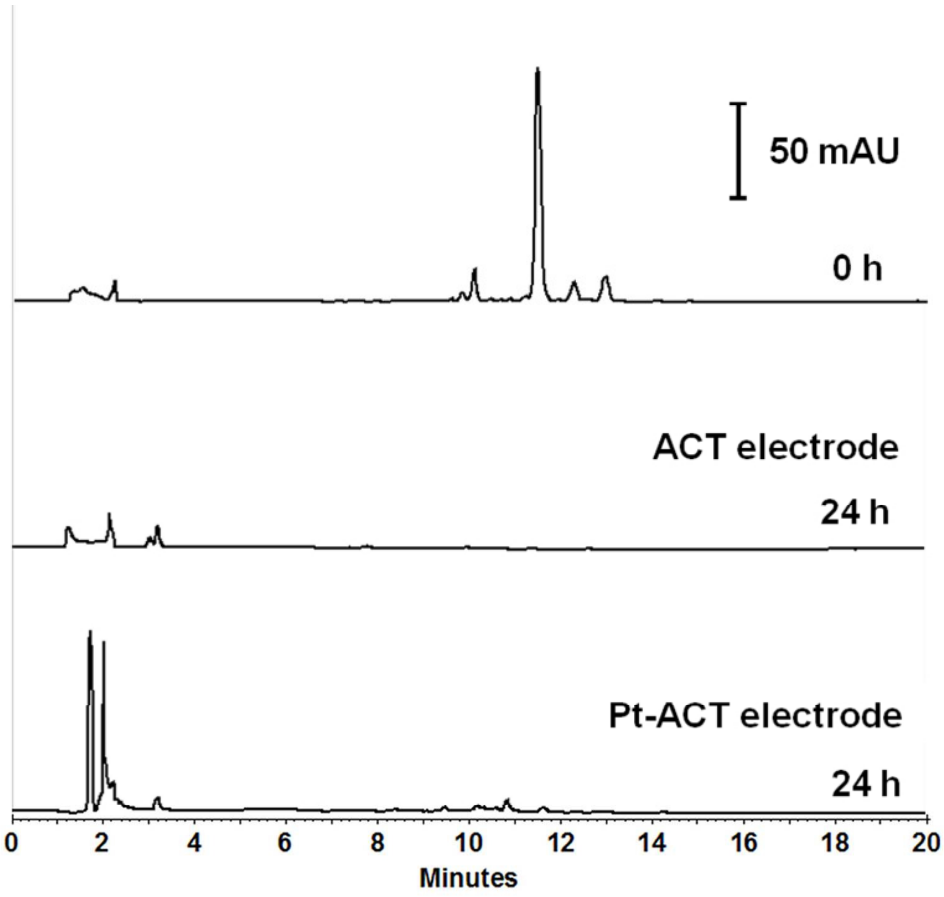

Figure 7 Chromatograms recorded at 310 nm before and after 24 hours of electrolysis performed with an ACT electrode and a Pt-ACT electrode.

72x67mm (300 x 300 DPI)

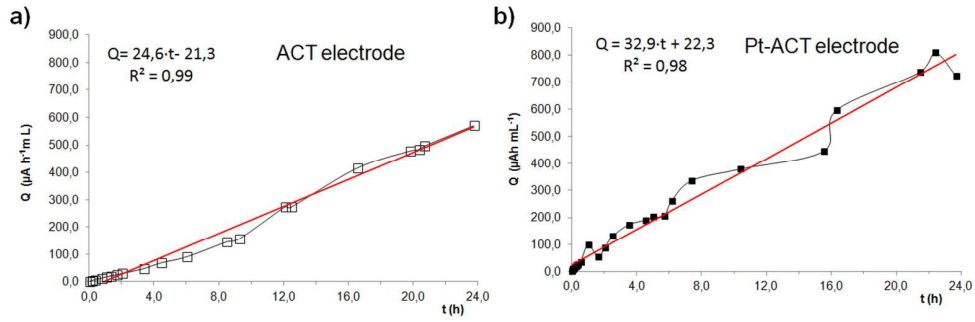

Figure 8 a) Specific applied charge evolution during the electrolysis with an ACT electrode at -0.10 V; b) Specific applied charge evolution during the electrolysis with a Pt-ACT electrode at 1.45 V in the presence of 0.3 g dm-3 NaCl.
277x89mm (118 x 118 DPI)

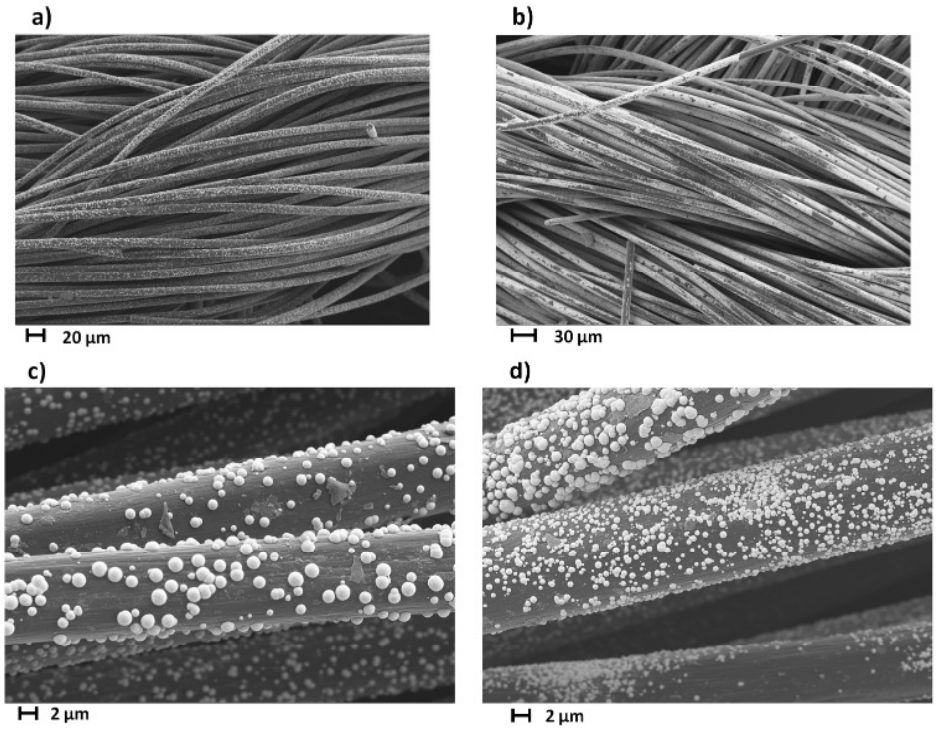

Figure 9 FESEM micrographs obtained before (a, c) and after 24h of electrolysis (b, d) of a 0.06 g dm-3 RMZB in 49 g dm-3 H_2SO_4 solution with a Pt-ACT electrode in the presence of 0.3 g dm-3 NaCl.